

PROTON DECAY FROM ISOBARIC ANALOG STATES FORMED IN THE  $(d, n)$  REACTIONS\*

N. Cue, P. Richard, and J. S. Blair  
University of Washington, Seattle, Washington  
(Received 26 June 1967)

A study of the cross sections of proton decay of isobaric analog states formed in the  $(d, n)$  reaction has been made with a variety of medium mass targets. Particular attention is paid to the large variation in cross sections for reactions which proceed through the analogs of  $d_{5/2}$ ,  $s_{1/2}$ , and  $d_{3/2}$  states in the Zr, Mo, and Sn isotopes. At energies ( $E_{\text{inc}} \sim 16$  MeV) far above threshold this variation is shown to be consistent with a sequential process in which the  $(d, n)$  formation mechanism is direct. The cross sections to the target ground states are large only when the neutron decay channels are closed.

Recently, decay protons from isobaric analog states (IAS) in  $\text{Nb}^{91*}$  have been observed following both  $(p, n)$  and  $(d, n)$  reactions.<sup>1,2</sup> These observations have motivated us to measure the cross sections for proton decay of IAS formed through the  $(d, n)$  reaction with a large number of different target nuclei. It was our initial hope that the branching ratios and other characteristics of the decay of IAS could be easily studied with this reaction. As the investigation has proceeded, however, we have learned that the  $(d, np)$  process is very selective and that the cross sections are large for only a few transitions. The purpose of this Letter is to show that the large variation in the magnitude of the  $(d, np)$  cross sections can be quite simply understood, even though our detailed understanding of the formation mechanism is incomplete.

The incident deuteron beam was obtained from the University of Washington's High Voltage Engineering Corporation Model FN tandem Van de Graaff accelerator. A  $\Delta E$ - $E$  detector telescope having a combined energy resolution of about 34 keV (full width at half-maximum) was used to detect 2- to 10-MeV protons. The targets investigated were self-supporting foils of  $\text{Y}^{89}$ ,  $\text{Zr}^{90,91,92,94}$ ,  $\text{Mo}^{92,94,98}$ , and  $\text{Sn}^{114,116,118,120}$ , as well as  $\text{Al}^{27}$ ,  $\text{Ni}^{64}$ ,  $\text{Zn}^{68}$ , and  $\text{Pb}^{206}$ . Our measurements consisted of excitation functions ( $\theta_{\text{lab}} = 170^\circ$ ) with the deuteron energy ranging from the  $(d, n)$  threshold of the ground-state analog (typically  $\sim 7$  MeV) to about 16 MeV, and angular distributions at various incident energies.

In general, proton yield from IAS is observed for all targets studied except  $\text{Mo}^{98}$ ,  $\text{Sn}^{118,120}$ , and  $\text{Pb}^{206}$ . A proton spectrum is shown in Fig. 1(a) for the case of a  $\text{Mo}^{92}$  target. One noteworthy feature at the higher incident energies is that the decay peaks fall near the maximum end of the energy range allowed by kinematics,

e.g.,  $[p_{00}]$  in Fig. 1(a), implying that the corresponding  $(d, n)$  angular distributions are forward peaked. The measured excitation functions exhibit a sharply rising cross section above threshold as is typified by the transition from the  $d_{5/2}$  IAS to the  $0^+$  ground state  $[p_{00}]$

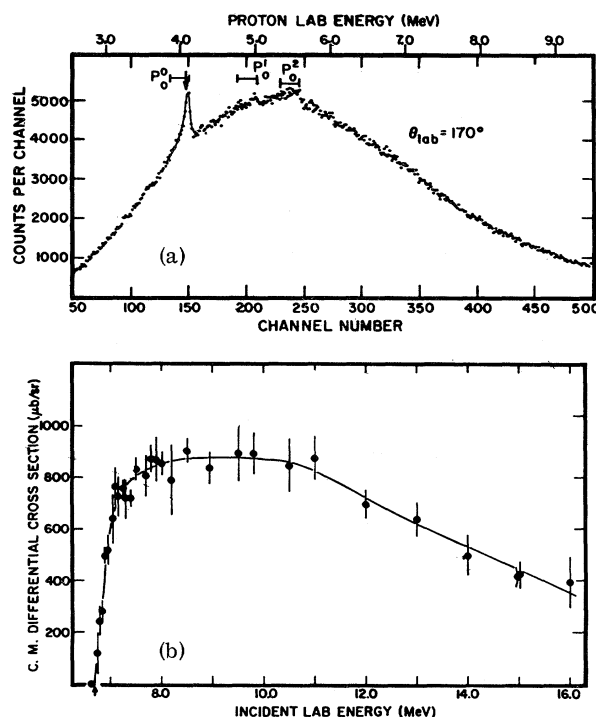


FIG. 1. (a) Proton spectrum following deuteron bombardment of  $\text{Mo}^{92}$  at 14.99-MeV proton energy. The only prominent peak in the spectrum is  $[p_{00}]$ , the  $d_{5/2}$  ground-state IAS decay to the  $0^+$  ground state of  $\text{Mo}^{92}$ . The horizontal line represents the energy range of the decay peak allowed by kinematics. (b) Excitation function at  $170^\circ$  for the  $p_{00}$  transition shown in (a). The  $(d, n)$  threshold for this transition is indicated by an arrow. The error bars include contributions from the counting statistics and the uncertainties in the estimation of background under the decay peak. The curve through the data points is merely to indicate the general trend.

from  $\text{Tc}^{93*}$  shown in Fig. 1(b). The excitation function for the transition from the  $d_{5/2}$  IAS to the  $0^+$  ground state [ $p_{00}$ ] from  $\text{Nb}^{93*}$  has a similar shape but is a factor of 8 less in magnitude. These differences in magnitude are typical of our observations; indeed, the cross section for the decay from the  $d_{5/2}$  IAS to the ground state decreases by at least a factor of 50 in going from  $\text{Tc}^{93*}$  to  $\text{Tc}^{99*}$ . We attempt to understand these variations on the basis of the following considerations.

Since the IAS have relatively narrow widths ( $\Gamma \lesssim 70$  keV), we may assume the  $(d, np)$  process to be sequential when the outgoing neutron energy is several times larger than  $\Gamma$ . The character of the measured angular distributions for the subsequent proton decay supports this assumption. The total cross section for proton decay to a given final state  $\sigma(d, np_{c'})$  may then be written as

$$\sigma(d, np_{c'}) = \sigma(d, n) G_{c'}, \quad (1)$$

where  $\sigma(d, n)$  is the total cross section for the formation of the IAS through the  $(d, n)$  reaction and  $G_{c'}$  is the branching ratio for the proton decay via channel  $c'$ .

In the case of decay to the ground state  $c' = c$ ,  $G_c$  is given by

$$G_c = (\Gamma_c + WP_c) / \Gamma, \quad (2)$$

where  $\Gamma$  is the total width and  $\Gamma_c$  is the partial width of the IAS as deduced from proton elastic-scattering experiments,  $W$  is the spreading width<sup>3</sup> for mixing of the IAS into the normal states, and  $P_c$  is the probability for subsequent proton decay of such normal states through channel  $c$ . In the case of decay to excited states,  $G_{c'}$  is given by

$$G_{c'} = \Gamma_{c'} / \Gamma, \quad (3)$$

where the partial width  $\Gamma_{c'}$  as deduced from the analysis of proton inelastic scattering includes implicitly the width for the roundabout decay through the normal states as well as the width for immediate decay of the IAS into exterior channel  $c'$ .

It is clear that the product  $WP_c$  in Eq. (2) can become very important when the neutron decay channels are closed. In this case it is often true that proton decay to the ground state is greatly favored over decay to excited states because of the respective barrier penetrabil-

ities; thus if the neutron channel is closed,  $G_c$  approaches unity.

If it is assumed that  $\sigma(d, n)$  can be estimated by means of the standard distorted-wave Born approximation (DWBA) model,<sup>4</sup> we can then write

$$\sigma(d, np_{c'}) = \left\{ \frac{(2J_A + 1)}{(2J_0 + 1)} \frac{S_{dp}}{(2T_0 + 1)} G_{c'} \right\} \sigma_{sp}(l), \quad (4)$$

where  $J_A$  is the spin of the IAS,  $J_0$  and  $T_0$  are, respectively, the spin and isospin of the target nucleus,  $S_{dp}$  is the spectroscopic factor deduced from analysis of the  $(d, p)$  stripping reaction leading to the parent of the IAS, and  $\sigma_{sp}(l)$  is the total single-particle cross section<sup>4</sup> for adding a proton of orbital angular momentum  $l$ . But even in situations where the  $(d, n)$  cross section is inadequately described by the DWBA theory, it may be reasonable to assume that the cross section will be proportional to the same spectroscopic and statistical factors contained within the bracket of Eq. (4). This quantity in brackets will be termed the enhancement factor,  $F_{c'}$ .

In Fig. 2 we display the calculated  $F_c$  factors and the angle-integrated cross sections<sup>5</sup> at the higher incident energies ( $\sim 16$  MeV) for the ground-state transitions from the analog of  $2d_{5/2}$ ,  $3s_{1/2}$ , and  $2d_{3/2}$  states in the Zr, Mo, and Sn isotopes. In the calculations of  $F_c$ , we have taken the values for  $\Gamma_c$ ,  $\Gamma$ , and  $S_{dp}$  from the literature.<sup>6,7</sup> Further, we have used  $G_c = 1$  when the neutron channel is closed and there is no evidence for decay to excited states, and  $G_c = \Gamma_c / \Gamma$  when the neutron channel is open. The scales are matched so that the  $F_c$  factors agree with the measured cross sections for the three strongest transitions from the  $d_{5/2}$  IAS to the  $0^+$  ground state; i.e.,  $\sigma(d, np_c) = 8.2 F_c$  mb. This value, 8.2 mb, is then the experimental single-particle cross section  $\sigma_{sp}(l=2)$  of Eq. (4) and is within the range predicted by the standard DWBA calculations that we have performed. Further, the fact that the experimental single-particle cross sections are almost independent of  $l$  and  $A$  is consistent with the DWBA calculations.<sup>8</sup> For the other targets studied, the largest  $(d, np)$  cross sections occur for cases where  $F_c$  is large. A more quantitative analysis is not yet completed.

We conclude from the comparisons made in Fig. 2 that the enhancement factors large-

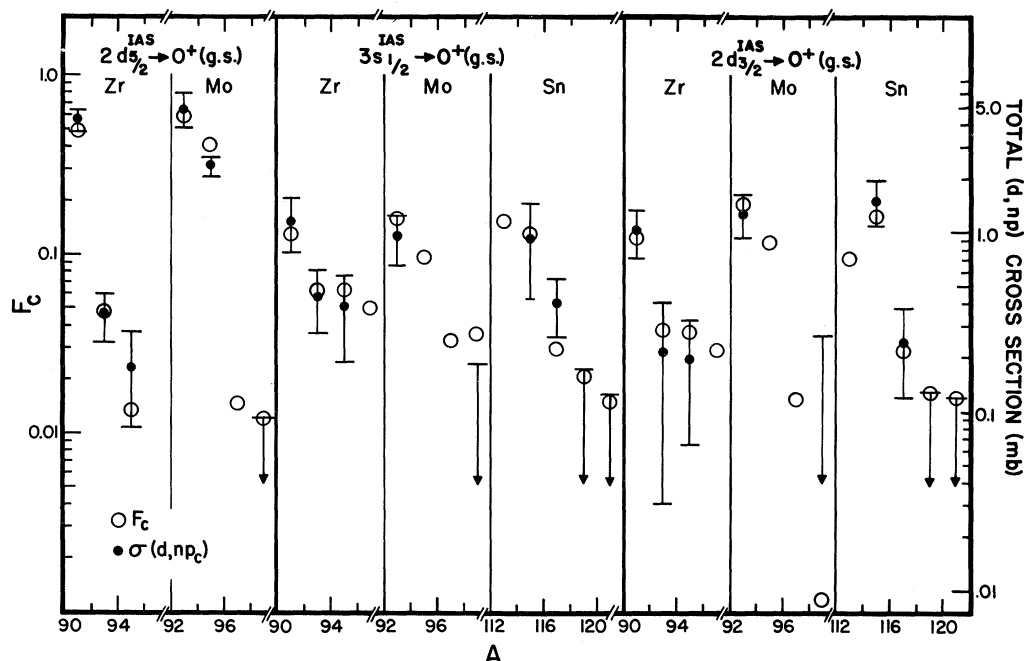


FIG. 2. The enhancement factors  $F_C$  (open circles) and the estimated angle-integrated cross section  $\sigma(d, np_C)$  (closed circles), obtained at the higher incident energies ( $\sim 16$  MeV), are shown for the cases of ground-state transitions from the analogs of  $2d_{5/2}$ -,  $3s_{1/2}$ -, and  $2d_{3/2}$ - states in the odd isotopes of Zr, Mo, and Sn (even-isotope targets). The arrows represent upper limit estimates of  $(d, np)$  cross sections. The scales are matched so that  $\sigma(d, np_C) = 8.2F_C$  mb for all transitions. The factors  $F_C$  for the analogs of states in  $Zr^{97}$ ,  $Mo^{97}$ , and  $Sn^{113}$  are included for the sake of completeness although the corresponding targets were not studied. The experimental cross sections for the analogs of  $s_{1/2}$  and  $d_{3/2}$  states in  $Mo^{95}$  are not shown because the corresponding decay peaks overlap with each other.

ly account for the variation in the observed  $(d, np)$  cross sections at the higher incident energies. As mentioned previously, the cross sections to the target ground states depend critically on whether or not the IAS can decay by neutron emission. This is clearly illustrated in the comparison of cross sections from analogs of states in  $Zr^{91}$  and  $Zr^{93}$  with the same  $J_A$ .

The shape of the observed excitation functions is not understood at present. Presumably the difficulty lies in the proper treatment of the formation mechanism. However, the  $F_C$  factors do seem to account for the relative variation in the magnitude of the  $(d, np)$  cross sections at the lower incident energies [ $\geq 1$  MeV above the  $(d, n)$  thresholds] although the agreement is not as good as that obtained at the higher energies.

Finally, we would like to comment that the original hope of using the  $(d, np)$  process to obtain accurate spectroscopic information will not be easily realized. The reasons are as follows: For most transitions (including de-

cay to all excited states) where the branching ratios  $G_C = \Gamma_C / \Gamma$  contain worthwhile spectroscopic information, the cross sections tend to be small and of the same magnitude as the other structure in the continuum background. The moderately large cross sections correspond mainly to ground-state transitions of IAS whose neutron-decay channels are closed; for these cases, the branching ratio  $G_C$  approaches unity independently of the elastic partial width.

\*Work supported in part by the U. S. Atomic Energy Commission.

<sup>1</sup>A. I. Yavin, R. A. Hoffswell, L. H. Jones, and F. M. Noweir, Phys. Rev. Letters **16**, 1049 (1966).

<sup>2</sup>C. F. Moore, C. E. Watson, S. A. A. Zaidi, J. J. Kent, and J. G. Kulleck, Phys. Rev. Letters **17**, 926 (1966).

<sup>3</sup>D. Robson, J. D. Fox, P. Richard, and C. F. Moore, Phys. Letters **18**, 86 (1965).

<sup>4</sup>R. H. Bassel, R. M. Drisko, and G. R. Satchler, Oak Ridge National Laboratory Report No. ORNL-3240, 1962 (unpublished).

<sup>5</sup>The angle-integrated cross sections were estimated

as follows: For decay from  $s_{1/2}$  IAS, this is simply  $4\pi$  times the  $170^\circ$  cross section. For decay from some of the  $d_{5/2}$  IAS to  $0^+$  ground state, the angular distributions have been measured at sufficient energies to allow us to extract a meaningful angle-integrated cross section at all energies studied; for the weaker transitions from  $d_{5/2}$  IAS, we have assumed that the angular distributions are the same as those measured for the stronger transitions at corresponding values of the outgoing neutron energy. Only one angular distribution has been measured for the decay of a  $d_{3/2}$  IAS to  $0^+$  state; this, together with some information concerning the  $m$ -substate populations of the IAS, has been used in converting the measured values for  $170^\circ$  cross section into rough estimates of angle-integrated cross sections.

<sup>6</sup>J. D. Fox, private communication; C. F. Moore, P. Richard, C. E. Watson, D. Robson, and J. D. Fox, Phys. Rev. **141**, 1166 (1966); P. Richard, C. F. Moore, J. A. Becker, and J. D. Fox, Phys. Rev. **145**, 971 (1966).

<sup>7</sup>B. L. Cohen and O. V. Chubinsky, Phys. Rev. **131**, 2184 (1963); S. A. Hjorth and B. L. Cohen, Phys. Rev. **135**, B920 (1964); E. J. Schneid, A. Prakash, and B. L. Cohen, Phys. Rev. **156**, 1316 (1967).

<sup>8</sup>We recognize that the standard DWBA theory is not really appropriate to cases in which a nucleon is captured into an unbound orbital. In our calculations, several bound-state form factors were considered with proton binding energies varying from essentially 0 to 7.2 MeV.

### SINGLE-PARTICLE PROTON STATES IN $^{209}\text{Bi}$ EXCITED IN THE $(^3\text{He}, d)$ REACTION\*

R. Woods, P. D. Barnes, E. R. Flynn, and G. J. Igo

Los Alamos Scientific Laboratory, University of California, Los Alamos, New Mexico

(Received 10 July 1967)

The position of the unperturbed neutron and proton single-particle levels in nuclei is fundamental to many nuclear structure calculations. Although the position of the neutron levels is reasonably well established, it is only recently that proton-stripping reactions have been used for this purpose. We report here a search for single-proton levels outside the doubly magic nucleus  $^{208}\text{Pb}$  using the  $(^3\text{He}, d)$  proton-stripping reaction.

The target was a self-supporting  $^{208}\text{Pb}$  foil 200  $\mu\text{g}/\text{cm}^2$  thick. A 24-MeV  $^3\text{He}$  beam from the Los Alamos tandem Van de Graaff facility was brought into the scattering chamber of a magnetic spectrograph of the Elbek design. The reaction products were analyzed with a deuteron resolution of  $\sim 25$  keV. Exposures were made at 20, 30, and  $45^\circ$ , and a typical spectrum is shown in Fig. 1. The numbered peaks refer to states in  $^{209}\text{Bi}$  and are listed in Table I.

The levels in  $^{209}\text{Bi}$  have also been studied by the inelastic scattering reactions  $(n, n')$ ,<sup>1</sup>  $(p, p')$ ,<sup>2</sup>  $(d, d')$ ,<sup>3</sup> and  $(\alpha, \alpha')$ ,<sup>4</sup> as well as in the low-resolution (170-keV) proton-stripping  $(\alpha, t)$  measurements of Stein and Lilley.<sup>5</sup> A comparison of the levels observed in these reactions with the present work is given in Table I. All levels above 3.8 MeV are unbound levels.

The deuteron spectrum of Fig. 1 is characterized by several strongly excited levels spread over 4 MeV of excitation. If we assume that these are of a single-particle character, then

it is of interest to compare their excitation energies with the predictions of a proton bound in a static potential well. Such calculations have been performed by several authors<sup>6-8</sup> for the bound proton orbitals,  $1h_{9/2}$ ,  $2f_{7/2}$ , and  $1i_{13/2}$ . In addition, Schröder<sup>7</sup> also estimates the position of a bound  $2f_{5/2}$  orbit. Recently, Korotkikh, Moskovkin, and Yudin<sup>9</sup> have extended these calculations of single-particle levels into the continuous spectrum using the Woods-Saxon well parameters of Blomqvist and Wahlborn.<sup>8</sup> A comparison of these various calculations with the observed single-proton spectrum is given in Fig. 2. Here all the spectra have been normalized on the  $1h_{9/2}$  level. The first two excited states presumably correspond to the  $2f_{7/2}$  and  $1i_{13/2}$  orbits and are in good agreement with the excitation-energy prediction of Blomqvist-Korotkikh<sup>8,9</sup> calculations, but are below the predictions of Schröder.<sup>7</sup> Of the three remaining orbits the unbound level at 4.425 MeV probably corresponds to the highest orbit in this shell, i.e., the  $3p_{1/2}$  orbit. The identification of the two bound levels at 2.821 and 3.643 MeV is not clear. The splitting of the  $f_{7/2}$ - $f_{5/2}$  orbits suggested by Schröder<sup>7</sup> is consistent with the 2.832-MeV level being the  $2f_{5/2}$  orbit. On the other hand, Korotkikh, Moskovkin, and Yudin<sup>9</sup> predict the  $p_{3/2}$  orbit to be below the  $f_{5/2}$  orbit with both being unbound levels.

Using the spin assignments suggested by Fig. 2, it is of interest to compare the observed